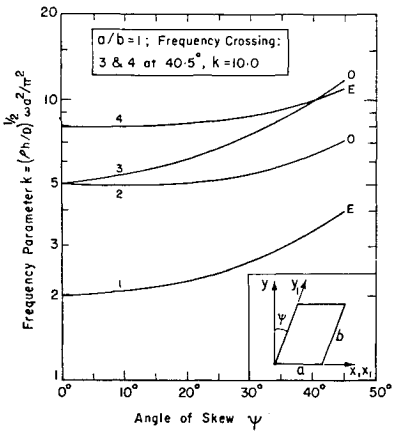

a) $a/b = 1$

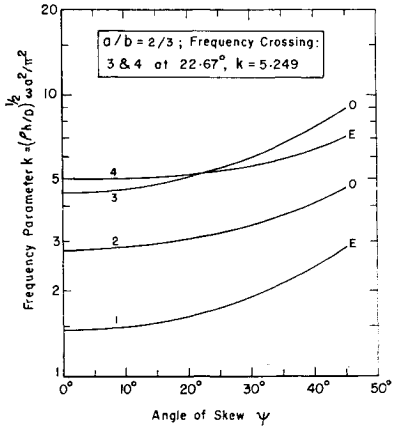

b) $a/b = \frac{2}{3}$

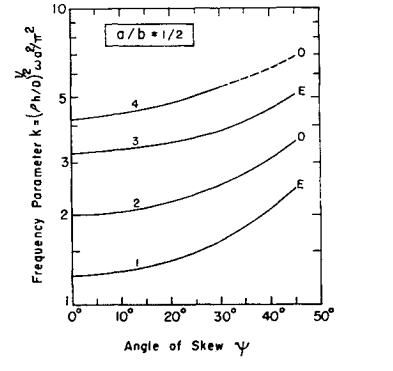

c) $a/b = \frac{1}{2}$

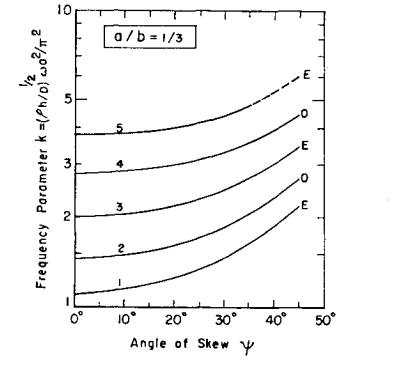

d) $a/b = \frac{1}{3}$

Fig. 1 Variation of natural frequencies with angle of skew.

system. Figure 1d shows the variation of the frequencies of of the first five modes for $a/b = \frac{1}{3}$.

It is interesting to observe that, while the skew angle tends to split the degeneracies of the modes of rectangular plates on one hand, it does bring about other degeneracies between different modes at certain other values corresponding to the frequency crossings. That is to say, the frequency crossings are degeneracies, since two different modes have the same frequency. Further, one observes that the frequency crossings are always between a pair of modes belonging to the opposite groups, even and odd.

References

[1] Durvasula, S., "Vibration and Buckling of Isotropic Parallelogrammic Flat Plates," paper presented at the 17th Annual General Meeting of the Aeronautical Society of India, Bangalore, April 9–10, 1965.

[2] Conway, H. D. and Farnham, K. A., "The Free Flexural Vibrations of Triangular, Rhombic and Parallelogram Plates and Some Analogies," *International Journal of Mechanical Sciences*, Vol. 7, No. 12, Dec. 1965, pp. 811–816.

[3] Gould, S. H., *Variational Methods for Eigenvalue Problems*, Mathematical Expositions 10, University of Toronto Press, Toronto, 1957, Chap. VI, p. 105.

[4] Collatz, L., *Numerical Treatment of Differential Equations*, Springer-Verlag, Berlin, 1960, Chap. 5, p. 395.

[5] Conway, H. D., "Analogies between the Buckling and Vibration of Polygonal Plates and Membranes," *Canadian Aeronautical Journal*, Vol. 6, No. 9, Sept. 1960, p. 263.

[6] Weinstein, A., "Some Numerical Results in Intermediate Problems for Eigenvalues," *Numerical Solution of Partial Differential Equations*, edited by J. H. Bramble, Academic Press, New York, 1966, pp. 167–191.

[7] Stadter, J. T., "Bounds to Eigenvalues of Rhombical Membranes," APL/JHU CF-3084, 1964, Applied Physics Lab., Johns Hopkins University, Silver Spring, Md.

[8] Durvasula, S., "Flutter of Simply Supported Parallelogrammic Flat Panels in Supersonic Flow," *AIAA Journal*, Vol. 5, No. 9, Sept. 1967, pp. 1668–1673.

[9] Durvasula, S., "Free Vibration of Simply Supported Parallelogrammic Plates," Rept. (under preparation), 1968, Department of Aeronautical Engineering, Indian Institute of Science, Bangalore.

[10] Claassen, R. W. and Thorne, C. J., "Vibrations of Thin Rectangular Isotropic Plates," *Journal of Applied Mechanics*, Vol. 28, No. 2, June 1961, pp. 304–305.

[11] Claassen, R. W. and Thorne, C. J., "Vibrations of a Rectangular Cantilever Plate," *Journal of the Aerospace Sciences*, Vol. 29, No. 11, Nov. 1962, pp. 1300–1305.

[12] Barton, M. V., "Vibration of Rectangular and Skew Cantilever Plates," *Journal of Applied Mechanics*, Vol. 18, No. 2, June 1951, pp. 129–134.

[13] Argyris, J. H., "Continua and Discontinua," *Matrix Methods in Structural Mechanics*, Proceedings of the Conference held at Wright-Patterson Air Force Base, Ohio, Oct. 26–28, 1965, AFFDL-TR-66-80, Nov. 1966, Air Force Flight Dynamics Laboratory, Wright-Patterson Air Force Base, Ohio.

Maximum Stress of a Stiffened Circular Cylinder under Bending

Tsai-Chen Soong*
The Boeing Company, Seattle, Wash.

Nomenclature

A_s = cross-sectional area of the stringer, in.²
d = stringer spacing, in.
E = Young's modulus of the skin, psi
h = distance from the neutral axis to the center of the cylinder, in.
M = bending moment, lb.-in.
R = radius of the circular cylinder, in.
t = skin thickness, in.

Received April 25, 1968; revision received August 26, 1968. The author thanks Chun Li of The Boeing Company for his help in the programming.

* Research Specialist A, Stress Analysis Research, Structures Staff, Commercial Airplane Division.

β = angle defined in Eq. (4), rad
σ_o = the true compressive stress at the crown, psi
$\bar{\sigma}_o$ = compressive stress defined in Eq. (1), psi
θ = the circumferential coordinate, rad

Introduction

THE von Kármán equation[1] of the effective width of a skin panel in uniaxial compression is often used to calculate the bending moment applied on a stiffened shell section when the maximum strain or stress at the crown of the compressed part of the shell is known. Even though the principle is simple, the actual application is a time-consuming process, because the effective width of the skin associated with a stringer is inversely proportional to the square-root of the local compressive stress and, as a consequence, the position of the neutral axis varies with the magnitude of the applied moment. For noncircular sections or circular section with nonuniform stringer-spacing, a cut-and-try method seems to be the only resort. Even in the simple case of circular section with uniform spacing, tabulations of solutions are not practical because the number of stringers has to be specified in each case before a functional relationship between the bending moment and the compressive stress at the crown can be established. This difficulty has been demonstrated in the Appendix.

The present analysis treats the circular shell with uniform stringers as an equivalent cylinder of variable thickness, and found that there are only two nondimensional parameters involved in its solution. One is A_s/td and the other is $(t/d)^2(E/\bar{\sigma}_o)$, where $\bar{\sigma}_o$ is the lower bound of the true crown stress obtained by assuming that the skin is fully effective in compression and the neutral axis coincides with the diameter of the cylinder. The true stress is then determined when these two parameters are given. Curves have been prepared for quick reference.

Derivations

If the skin of a thin-walled circular cylindrical shell with equally spaced constant stringers is fully effective under compressive load, the maximum compressive stress for a pure bending moment applied to the cylinder is

$$\bar{\sigma}_o = M \Big/ \left[4R^2 \int_0^{\pi/2} \left(t + \frac{A_s}{d} \right) \cos^2\theta d\theta \right] = M \Big/ \left[\pi R^2 \left(t + \frac{A_s}{d} \right) \right] \quad (1)$$

where the area of a stringer is averaged on its spacing. Figure 1 shows notations of the idealized stiffened cylinder in which the upper part is assumed to be in compression under the bending moment.

The stress represented by Eq. (1), however, is only a lower bound of the true maximum stress because the discreteness of the stringers caused the unsupported part of the skin to be less efficient in compression than the skin which is closer to the stringers. In fact, the usual practice in design is to take a certain width of the skin as an integral part of the stringer and neglect the rest. The so-called "effective" width of the skin can be represented by the following equation[1]:

$$W_e = 1.7t(E/\sigma)^{1/2} \quad (2)$$

where σ is the local compressive stress within the elastic limit. The numerical coefficient 1.7 is commonly used in design rather than the theoretical value, which is 1.9 approximately.

Assuming that plane sections remain plane in bending, the stress at any point of coordinate θ is

$$\sigma = \sigma_o \frac{(\cos\theta + h/R)}{(1 + h/R)} \quad (3)$$

Since the effective width is, at most, equal to the spacing of the stringers, there is a portion of the skin just above the neutral axis for which all of the skin is effective in compression. This angle, named β in Fig. 1, is determined in the following equation:

$$\cos\beta = (E/\sigma_o)(1 + h/R)(1.7t/d)^2 - h/R \quad (4)$$

The bending moment on the section can be calculated as

$$\frac{M}{2\sigma_o R^2 t} = \frac{1 + A_s/td}{1 + h/R} \left[\int_0^{(\pi/2) - \sin^{-1}(h/R)} \left(\cos\phi - \frac{h}{R} \right)^2 \times d\phi + \int_0^{(\pi/2) + \sin^{-1}(h/R)} \left(\cos\theta + \frac{h}{R} \right)^2 d\theta \right] - \int_0^{\beta} \frac{(\cos\theta + h/R)^2}{1 + h/R} d\theta + \frac{1.7t}{d} \left[\frac{E}{\sigma_o(1 + h/R)} \right]^{1/2} \times \int_0^{\beta} \left(\cos\theta + \frac{h}{R} \right)^{3/2} d\theta \quad (5)$$

Substitution of Eqs. (4) and (5) into (1), followed by integration, yields

$$\frac{\bar{\sigma}_o}{E} \left(\frac{d}{1.7t} \right)^2 = \left[\frac{\pi}{2} \left(1 + \frac{A_s}{td} \right) \left(\cos\beta + \frac{h}{R} \right) \right]^{-1} \times \left\{ \left(1 + \frac{A_s}{td} \right) \pi \left(\frac{1}{2} + \frac{h^2}{R^2} \right) - \left[\frac{1}{2} + \left(\frac{h}{R} \right)^2 \right] \beta - \frac{2h}{R} \sin\beta - \frac{1}{4} \sin 2\beta + \left(\cos\theta + \frac{h}{R} \right)^{1/2} J_1 \right\} \quad (6)$$

where the quantity J_1 is defined as

$$J_1 = \int_0^{\beta} \left(\cos\theta + \frac{h}{R} \right)^{3/2} d\theta \quad (7)$$

and can be reduced to a sum of elliptic integrals. The final result is

$$J_1 = \left\{ \left[\frac{(2)^{1/2}}{3} - \left(\frac{4(2)^{1/2}}{3} \right) \left(\frac{h}{R} \right) + (2)^{1/2} \left(\frac{h}{R} \right)^2 \right] \times F\left(\gamma, \frac{1}{r} \right) + 8(2)^{1/2} \left(\frac{1}{3} \right) \left(\frac{h}{R} \right) \cdot E\left(\gamma, \frac{1}{r} \right) + \left(\frac{2}{3} \right) \sin\theta \left(\cos\theta + \frac{h}{R} \right)^{1/2} \right\} \Bigg|_0^{\beta} \quad (8)$$

where

$$\gamma = \sin^{-1} \left(\frac{1 - \cos\theta}{1 + h/R} \right)^{1/2} \qquad r = \left[\frac{2}{(1 + h/R)} \right]^{1/2} \quad (9)$$

and

$$E\left(\gamma, \frac{1}{r} \right) = \int_0^{\gamma} \left[1 - \left(\frac{\sin\beta}{r} \right)^2 \right]^{1/2} d\beta = \int_0^{\sin\gamma} \left[\frac{(1 - x^2/r^2)}{(1 - x^2)} \right]^{1/2} dx \quad (10a)$$

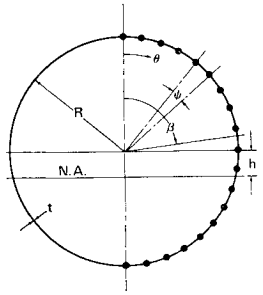

Fig. 1 Notations of the idealized section.

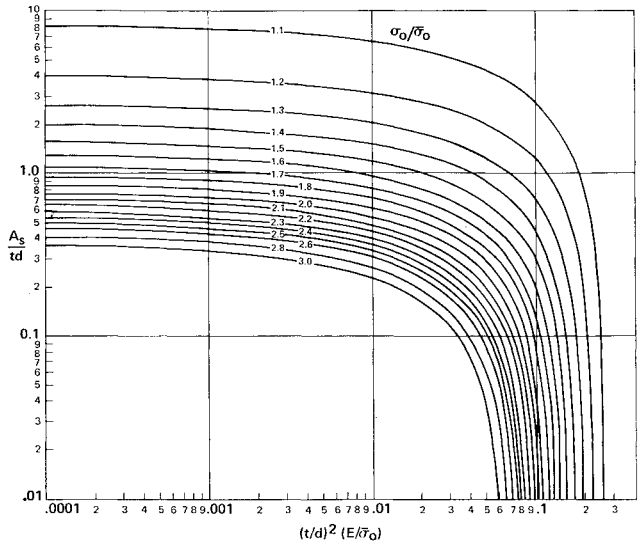

Fig. 2 Curves for stress ratios.

$$F\left(\gamma, \frac{1}{r}\right) = \int_0^{\gamma} \left[1 - \frac{\sin\beta}{r}\right)^2\Big]^{-1/2} d\beta$$
$$= \int_0^{\sin\gamma} \left[\frac{1 - x^2}{r^2}(1 - x^2)\right]^{-1/2} dx \quad (10b)$$

which are elliptic integrals of the second and the first kind, respectively. Their values are tabulated in various references.

Finally, the neutral axis can be determined by taking moments of the areas of the section about the neutral axis;

$$\int_0^{\beta} \left(\frac{1}{d}\right)(W_e t + A_s)\left(\cos\theta + \frac{h}{R}\right) d\theta + \int_{\beta}^{\pi} \left(t + \frac{A_s}{d}\right)\left(\cos\theta + \frac{h}{R}\right) d\theta = \quad (11)$$

After substitution of Eqs. (1–4) into (11) and integration, one obtains

$$1 + A_s/td = (\pi h/R)^{-1}[\sin\beta + \beta h/R - (\cos\beta + h/R)^{1/2} \cdot J_2] \quad (12)$$

where

$$J_2 = \int_0^{\beta} \left(\cos\theta + \frac{h}{R}\right)^{1/2} d\theta = (2)^{1/2}\left\{2E\left(\gamma, \frac{1}{r}\right) - \left(1 - \frac{h}{R}\right) F\left(\gamma, \frac{1}{r}\right)\right\}\Big|_0^{\beta} \quad (13)$$

The two quantities β, r, and the two elliptic integrals $E(,)$ and $F(,)$ are defined in Eqs. (9, 10a, and 10b).

Equations (6) and (12) contain two unknown quantities, β and h/R, against two nondimensional parameters, A_s/td and $(t/d)^2(E/\bar{\sigma}_o)$, which are known when the geometry of the cylinder and the applied moment are given. A CDC 6600 digital computer was used to solve Eqs. (6) and (12) for a wide range of shell geometry and bending moments. The results are plotted in Fig. 2, in which A_s/td is the ordinate, $(t/d)^2(E/\bar{\sigma}_o)$ is the abscissa and curves corresponding to constant values of $\sigma_o/\bar{\sigma}_o$, from 1.1 to 3.0, are drawn.

The accepted design approach assumes that the effective area of the skin is concentrated at the corresponding stringer and that the stringers are discrete elements. To compare the results of the present analysis with that approach, Eqs. (A1) and (A2), corresponding to Eqs. (6) and (12), are derived in the Appendix. Table 1 showed the results from these two sets of equations as based on an example with the following data input:

$R = 127.75$ in. $\quad t = 0.062$ in. $\quad M = 76 \times 10^6$ in.lb

$E = 10.5 \times 10^6$ psi $\quad A_s/d = 0.03244$ in.

$\bar{\sigma}_o = 15{,}692$ psi

It can be seen from Table 1 that, for three different stringer spacings, the results based on these two methods agree closely.

Appendix: Equations for Treating the Effective Skins as Discretely Connected to the Stringers

If the effective area of the skin is assumed to be concentrated at the corresponding stringers which are discrete along the circumference as in design practice, the bending moment equation, similar to Eq. (5), can be written as

$$\frac{M(1 + h/R)}{\sigma_o R} = 2tR \int_0^{(\pi/2) - \sin^{-1}(h/R)} \left(\cos\phi - \frac{h}{R}\right)^2 d\phi + A_s\left(1 - \frac{h}{R}\right)^2 + 2A_s\left[\sum_{n=1}^{N_1}\left(\cos n\psi - \frac{h}{R}\right)^2\right] + \left(1 + \frac{h}{R}\right)^2\left[A_s + 1.7t^2\left(\frac{E}{\sigma_o}\right)^{1/2}\right] + 2\sum_{n=1}^{N_2}\left(\cos n\psi + \frac{h}{R}\right)^2\left[A_s + 1.7t^2 \times \left(\frac{E(1 + h/R)}{\sigma_o(\cos n\psi + h/R)}\right)^{1/2}\right] + 2(A_s + d\cdot t) \times \sum_{n=1}^{N_3}\left[\cos(n + N_2)\psi + \frac{h}{R}\right]^2 \quad (A1)$$

where

ψ = angle in radians subtended by one stringer, see Fig. 1

N_1 = half the number of the stringers on the tension side of the section, omit the lowest stringer at $\theta = \pi$
= $[(\pi/2) - \sin^{-1}h/R)]/\psi$, to the nearest smaller integer

N_2 = half the number of the stringers on the compression side in which the effective width is less than the spacing, omit the top stringer at $\theta = 0$
= β/ψ, to the nearest smaller integer

N_3 = half the number of stringers for which the effective width is made to be equal to the spacing; = $\frac{1}{2}$ × number of stringers $- N_1 - N_2 - 1$

Equation (4) should be used to relate σ_o with β and h/R. For convenience, the number of stringers has been assumed to be an even integer in Eq. (A1) and there are stringers at $\theta = 0$ and π, respectively. The equation which defines the location of the neutral axis, similar to Eq. (11), is

$$2tR^2 \int_0^{(\pi/2) - \sin^{-1}(h/R)} \left(\cos\phi - \frac{h}{R}\right) d\phi + A_s R\left(1 - \frac{h}{R}\right) + 2A_s R\left[\sum_{n=1}^{N_1}\left(\cos n\psi - \frac{h}{R}\right)\right] - \left[A_s + 1.7t^2\left(\frac{E}{\sigma_o}\right)^{1/2}\right] R\left(1 + \frac{h}{R}\right) - 2R\sum_{n=1}^{N_2}\left(\cos n\psi + \frac{h}{R}\right)\left[A_s + 1.7t^2\frac{E(1 + h/R)}{\sigma_o(\cos n\psi + h/R)}\right)^{1/2}\Big] - 2R(A_s + d\cdot t)\sum_{n=1}^{N_3}\left[\cos(n + N_2)\psi + \frac{h}{R}\right] = 0 \quad (A2)$$

From Eqs. (A1) and (A2), the same problem can be solved provided the number of stringers is given. That the solution in this approach contains one more parameter than the present analysis can be seen by dividing Eqs. (A1) and (A2) by $t \cdot d$. The resulting equations have three parameters,

Table 1 Numerical comparison

d, in.	9.55567	6.37045	3.82227
A_s/td calculated	0.523249	0.523249	0.523249
$(t/d)^2(E/\bar{\sigma}_o)$ calculated	0.028168	0.063378	0.176051
Stress ratio:			
Based on Eqs. (6) and (12)	1.7742	1.5230	1.1672
Based on Eqs. (A1) and (A2)	1.7895	1.5353	1.1693
Ratio of results based on these two methods	0.9915	0.9920	0.9982

A_s/td, $(t/d)^2(E/\bar{\sigma}_o)$, and R/d. The last one is the number of stringers divided by 2π.

Reference

[1] von Kármán, T., Sechler, E. E., and Donnell, L. H., "The Strength of Thin Plates in Compression," *Transactions of the American Society of Engineering*, Vol. 54, 1932, p. 53.

"Power Law" Profiles in Thermally Stratified Shear Flows

HSING CHUANG*
University of Louisville, Louisville, Ky.
AND
JACK E. CERMAK†
Colorado State University, Fort Collins, Colo.

Nomenclature

c_p = Specific heat of air at constant pressure, cal/°C/gm
g = gravitational acceleration, cm/sec²
H = heat flux in the vertical direction, cal/cm²/sec
k = von Kármán constant
K_h = eddy thermal diffusivity, cm²/sec
K_m = eddy viscosity, cm²/sec
L = Monin-Obukhov length scale, $L' = (K_h/K_m)L = (Tu_*/gk)(\partial U/\partial z)/(\partial T/\partial z)$, cm
N = total number of data collected in a profile
R = dimensionless lapse rate, $(z/T_*)(\partial T/\partial z)$
Ri = $(g/T)(\partial T/\partial z)/(\partial U/\partial z)^2$, Richardson number
S = dimensionless wind shear, $(kz/u_*)(\partial U/\partial z)$
T = mean absolute temperature, °K
T_* = $-H/(c_p\rho k u_*)$, scaling temperature, °C
u_* = friction velocity, cm/sec
U = local mean velocity, cm/sec
z = height, cm
β, γ = arbitrary constants
ζ = z/L', dimensionless height
ρ = density of air, gm/cm³
$(\ )_i$ = the variable at height z_i
$(\ )_m$ = mean value averaged over the profile
$(\ )_0$ = the variable at height z_0, an equivalent roughness height

1. Introduction

THE historically old "power law" has recently been revived by Pandolfo.[1] His profile has $-\frac{1}{6}$ power instead of $-\frac{1}{3}$ power profile of free convection tested by Taylor.[2] He claimed that $-\frac{1}{6}$ power law described the observed wind profiles quite accurately and that his model was more accurate

Received May 20, 1968; revision received September 3, 1968.
Financial support provided by the U.S. Army through Research Grant DA-AMC-28-043-G20 for this study is gratefully acknowledged.

* Associate Professor, Department of Mechanical Engineering. Member AIAA.
* Professor-in-Charge, Fluid Mechanics Program, and Chairman, Department of Engineering Science. Member AIAA.

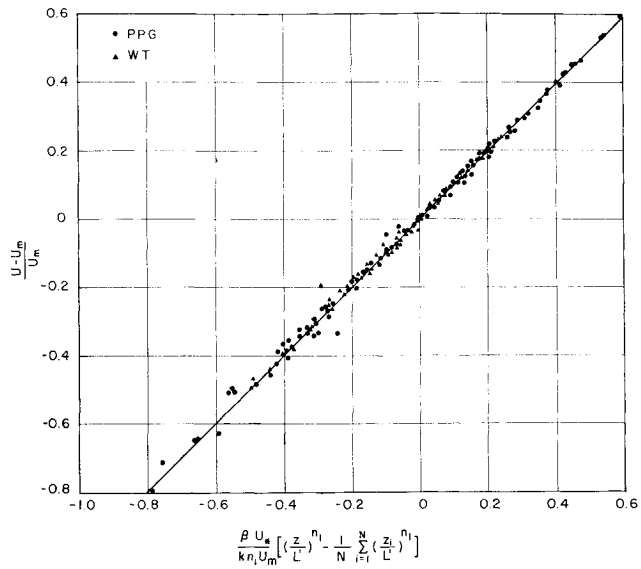

Fig. 1 Power law profile of the mean wind velocity.

to describe the wind profiles than Taylor's free convection model[2] or Swinbank's exponential model.[3] Pandolfo also compared his profile with KEYPS profile,[4] and concluded that these two models were comparable to each other pertaining to their accuracy of wind profiles description.

The mean velocity distribution in a neutral turbulent boundary layer is approximately given by Eq. (15) of Ref. 5 or Eq. (10) of Ref. 6. However, it is doubtful that the mean velocity distribution in thermally stratified shear flows will assume the same functional dependence on the height z as the neutral flow does. The power law model can indeed describe accurately the velocity profiles in thermally stratified shear flows. However, it is important to point out that the power should not be constant in all ranges of thermal stability, but rather dependent on the thermal stability as shown by Deacon[7] and should approach $-\frac{1}{3}$ profile as the flowfield approaches a free convection. The power profile is examined in this paper to show that this is the case for both laboratory and field data. Similarity between wind and temperature profiles is also studied.

2. Basic Equations

If the dimensionless wind shear and lapse rate are assumed to be proportional to ζ^n, then the mean wind velocity and the mean temperature will take the following forms:

$$U(z) - U_0(z_0) = (\beta u_*/kn)(\zeta^n - \zeta_0{}^n) \tag{1}$$

and

$$T(z) - T_0(z_0) = (\gamma T_*/n)(\zeta^n - \zeta_0{}^n) \tag{2}$$

The power n in the preceding equations should depend largely on the thermal stability of the flowfield. When data points are closely spaced and the respective velocity and temperature gradients in the vertical direction can be approximated by using finite difference techniques, the power n can be determined by the following equations:

$$\ln\frac{U_{i+1} - U_i}{z_{i+1} - z_i} = (n - 1)\ln\frac{z_{i+1} + z_i}{2} + \ln\frac{\beta u_*}{kL'^n} \tag{3}$$

and

$$\ln\frac{T_{i+1} - T_i}{z_{i+1} - z_i} = (n - 1)\ln\frac{z_{i+1} + z_i}{2} + \ln\frac{\gamma T_*}{L'^n} \tag{4}$$

where i varies from 1 to $N - 1$. If similarity between the velocity and the temperature profiles does not exist, then n will assume n_1 and n_2 in the preceding equations, respectively.